Multiple Classifiers Global Dynamic Fusion Location System based on WiFi and Geomagnetism

Feng Xu, Linfu Duan, Xiansheng Guo, Lin Li, and Fangzi Hu
Dept. Electronic Engineering
University of Electronic Science and Technology of China
Chengdu, China
Email: xsguo@uestc.edu.cn

***Abstract*—The existing WiFi and geomagnetism based positioning methods using single classifier show low accuracy because they are sensitive to changing environments. In this paper, we propose a global dynamic fusion location algorithm for multiple classifiers based on WiFi and geomagnetic fingerprints. In the offline phase, we first divide a positioning environment into some grid points and construct RSS and geomagnetic fingerprints for each grid point. Then, we train multiple classifiers by using the constructed fingerprints. Second, we derive a global dynamic fusion weight training method for each grid point through the global supervised optimization learning. In the online phase, given an RSS testing sample, we select the matching weights for fusion by using K-nearest neighbor (KNN). Our proposed multiple classifiers global dynamic fusion algorithm can make full use of the intrinsic complementarity of multiple classifiers, thus effectively improving the positioning accuracy of RSS and geomagnetic fingerprints. Experimental results show that the proposed algorithm outperforms some existing methods in complex indoor environments.**

***Index Terms*—Indoor position; WiFi; received signal strength (RSS), geomagnetism; machine learning**

I. Introduction

Indoor positioning has been gaining a lot of interest in recent years due to explosion in the number of smart devices and relevant technologies. It is relevant in shopping mall and museum and provides invaluable information for first responder. Accurate indoor location information can also help service provider to identify coverage holes and traffic hot spot when deploying networks of 4-G long-term evolution (LTE) small cells and WiFi access points (APs). In recent years, the fingerprint positioning method based on machine learning and deep learning [1–4] has achieved relatively satisfactory results in accuracy and robustness. The signal medium used in the positioning process is various, such as WiFi [1, 5, 6], RFID [7], geomagnetic field [4], inertial navigation [8], ultra-wideband[9] and ultrasonic wave[10], Bluetooth[11], etc. Among them, WiFi's high penetration rate and its easy-to-obtain nature make it an advantage in positioning. Geomagnetism is also becoming more and more popular among researchers because of its ubiquitous nature and relatively stable signals. However, the single algorithm or single fingerprint positioning accuracy cannot fully leverage the complementarity between each classifier.

To further improve the positioning accuracy, fusion of multiple classifiers is a popular solution in indoor localization [12, 13]. For example, Guo *et al.* first proposed the MUltiple Classifiers mUltiple Samples (MUCUS) based GrOup Of Fingerprints (GOOF) method to improve the accuracy of positioning in complex indoor environment by using multiple antenna platform [3]. In [14], the fusion weight matrix is dynamically generated for each grid point in the offline phase, and then the weight matrix is used to fuse multiple algorithm results in the online phase, however, the drawback of [14] is that it cannot make full use of the advantages of multiple algorithms. In [15, 16], we proposed the concept of the global fusion profile (GFP) based on WiFi received signal strength (RSS) and it can remarkable improve the accuracy of positioning in changing environment.

In recent years, fusion positioning is the best choice for stability and accuracy. The fusion location algorithm is mainly divided into two types, one is the fusion[17] on the data source, and the other is the fusion[14, 15] on the result set. This paper makes full use of these two fusion positioning ideas. In the data source, fusion of geomagnetism and WiFi fingerprints is performed. On the result set, an optimal fusion matrix is sought to obtain reliable positioning results.

The above methods just consider the positioning problem using RSS fingerprints, which cannot make full use of the environment information of the user. Geomagnetism is an efficient positioning metric to improve the accuracy of RSS fingerprints based methods. Zhang *et al.* proposed a deep learning based positioning method by fusing the geomagnetism and WiFi fingerprints for smart phone [4]. However, the article only calibrates geomagnetism and then stitches it directly to the WiFi signal. Bolat *et al.* proposed a hybrid indoor positioning solution based on WiFi, magnetic field, and inertial navigation to compensate for the inadequacy of a single sensor [8]. This paper first uses WiFi fingerprints to obtain a coarse location estimate; then, a particle filter algorithm is adopted to tracking a target based on magnetic field fingerprints. Fentaw *et al.* proposed a robust localization method by combining the modulus information of geomagnetism and inertial measurement units (accelerometers and gyroscopes) to avoid the fluctuation of the magnetic field.

Unlike the existing works, we propose a multiple classifiers global dynamic fusion location system based on WiFi and geomagnetic fingerprints. In the offline phase, firstly, a preprocessing method is used to align the two heterogeneous fingerprints. Then, several independent machine learning algorithms are selected to train multiple classifiers, and the global weighted matrix for each grid point is obtained through global supervised optimization learning. In the online phase, the final fusion coordinate position is obtained according to the global dynamic fusion algorithm.

II. Fingerprint Construction and Preprocessing

Assume a location environment can be divided into K grid points, and covered by M APs. We can construct magnetic and RSS fingerprints by using a smart phone for each grid point sequentially.

A. Construction of Geomagnetism and Calibration

Let $\boldsymbol{b}_k(n) = \left[b_x^k(n), b_y^k(n), b_z^k(n)\right]^T$ is an original three-dimensional magnetic magnitudes vector obtained by a smart phone at the n-th time instant at the k-th grid point ($n = 1, 2, \cdots, N; k = 1, 2, \cdots, K$ with N being the total number of the fingerprints at each grid point). Consider that the magnetic magnitudes vector is strongly dependent on directionality [18], so, we first calibrate it to eliminate the influence of direction [19, 20].

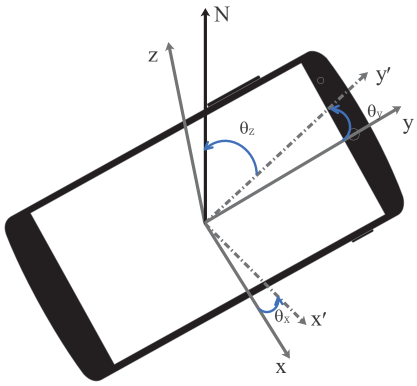

Fig. 1: The actual coordinate axis versus reference coordinate axis.

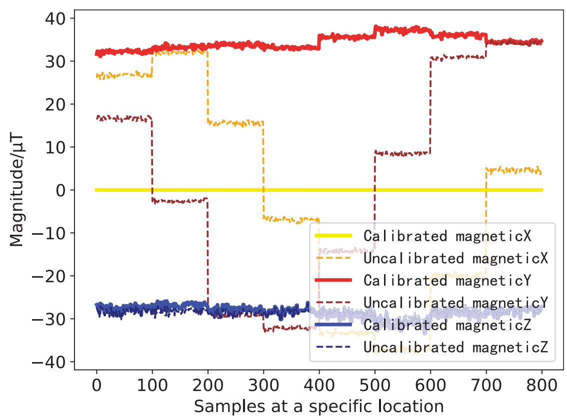

Fig. 2: Comparison of calibrated and uncalibrated magnetism.

Let $\left[\theta_x^k(n), \theta_y^k(n), \theta_z^k(n)\right]^T$ be the angle difference between the actual coordinate axis and the reference coordinate axis, measured at the n-th time instant at the k-th grid point, as shown in Fig. 1. Hence, we can obtain the calibrated magnetic data by the following formula:

$$\boldsymbol{m}_l(n) = \left[m_x^k, m_y^k, m_z^k\right]^T = \left[\boldsymbol{R}_x^k(n)\, \boldsymbol{R}_y^k(n)\, \boldsymbol{R}_z^k(n)\right]^{-1} \boldsymbol{b}_k(n), \tag{1}$$

where

$$\boldsymbol{R}_x^k(n) = \begin{bmatrix} 1 & 0 & 0 \\ 0 & \cos\left(\theta_x^k(n)\right) & -\sin\left(\theta_x^k(n)\right) \\ 0 & \sin\left(\theta_x^k(n)\right) & \cos\left(\theta_x^k(n)\right) \end{bmatrix},$$

$$\boldsymbol{R}_y^k(n) = \begin{bmatrix} \cos\left(\theta_y^k(n)\right) & 0 & -\sin\left(\theta_y^k(n)\right) \\ 0 & 1 & 0 \\ \sin\left(\theta_y^k(n)\right) & 0 & \cos\left(\theta_y^k(n)\right) \end{bmatrix},$$

and

$$\boldsymbol{R}_z^k(n) = \begin{bmatrix} \cos\left(\theta_z^k(n)\right) & -\sin\left(\theta_z^k(n)\right) & 0 \\ \sin\left(\theta_z^k(n)\right) & \cos\left(\theta_z^k(n)\right) & 0 \\ 0 & 0 & 1 \end{bmatrix}.$$

Fig. 2 shows the comparison of the calibrated and uncalibrated geomagnetism at a specific grid point. It can be seen that the calibrated geomagnetism has nothing with the directions. Any direction can be selected to collect geomagnetic data without considering the attitude of the mobile phone if we use the above calibration strategy.

B. Construction of WiFi RSS Fingerprints and Normalization

Let $\boldsymbol{r}_k(n) = \left[r_k^1(n), r_k^2(n), \cdots, r_k^M(n)\right]^T$ is the RSS vector collected at the n-th time instant at the k-th grid point. If an AP cannot detect the strength of its WiFi signal due to a weak cell phone signal, we manually give the corresponding AP a value of -110 dBm to ensure that all samples have the same dimension.

Denote $\boldsymbol{d}_k(n) = \left[d_k^1(n), d_k^2(n), \cdots, d_k^L(n)\right]^T = \left[\boldsymbol{m}_k^T(n), \boldsymbol{r}_k^T(n)\right]^T$ as the joint fingerprints combined the geomagnetism with the RSS, where $L = M + 3$. Since geomagnetism and WiFi are two different fingerprints, it is necessary to normalize the two kinds of data before fusion positioning to make both data have same range. We first calculate the mean and standard bias of the joint fingerprint $\boldsymbol{d}_k(n)$ as

$$\mu_l = \frac{1}{NK} \sum_{k=1}^{K} \sum_{n=1}^{N} d_k^l(n), \tag{2}$$

and

$$\sigma_l = \sqrt{\frac{1}{NK} \sum_{k=1}^{K} \sum_{n=1}^{N} \left(d_k^l(n) - \mu_l\right)^2}, \tag{3}$$

where $l = 1, 2, \cdots, L$. We can obtain the normalized vector for geomagnetism and RSS fingerprints as

$$\boldsymbol{d}^l = \frac{\boldsymbol{d}^l - \mu_l}{\sigma_l}. \tag{4}$$

III. The Proposed Positioning Algorithm

A. Classifiers Training

Our proposed localization framework is shown in Fig. 3. In the offline phase, the collected geomagnetism and RSS fingerprints $\boldsymbol{d}_k(n) = \left[d_k^1(n), d_k^2(n), \cdots, d_k^L(n)\right]^T = \left[\boldsymbol{m}_k^T(n), \boldsymbol{r}_k^T(n)\right]^T$ at the k-th grid point can be divided into two groups, i.e., $\boldsymbol{D}_k = [\boldsymbol{d}_k(1), \cdots, \boldsymbol{d}_k(Q)] \in \mathcal{R}^{L\times Q}$ and $\boldsymbol{D}'_k = [\boldsymbol{d}_k(Q+1), \cdots, \boldsymbol{d}_k(N)] \in \mathcal{R}^{L\times(N-Q)}$ with Q being an arbitrary integer between 2 and $N-1$ and N being the total number of fingerprints. The former is used to train classifiers and the latter is for weights training. The total training fingerprints $\boldsymbol{D} = [\boldsymbol{D}_1, \cdots, \boldsymbol{D}_K]$.

Assume that we have H different machine learning algorithms for classifiers training, denotes by $f_1(\cdot), \cdots, f_H(\cdot)$. Hence, we can obtain the trained classifiers, $f_1(\boldsymbol{D}), \cdots, f_H(\boldsymbol{D})$, by using the training fingerprints $\boldsymbol{D}$ in the offline phase.

B. Weights Training

After having obtained the trained multiple classifiers $f_1(\boldsymbol{D}), \cdots, f_H(\boldsymbol{D})$, we can get the predictions $\boldsymbol{z}_k^h$ of the h-th classifier ($h = 1, \cdots, H$) when giving the offline testing fingerprints $\boldsymbol{D}'_k$ at the k-th grid point, that is

$$\boldsymbol{z}_k^h = \left[z_k^h(1), \cdots, z_k^h(\mathcal{L})\right]^T \tag{5}$$

with $\mathcal{L} = N - Q$. The i-th prediction can be given by

$$z_k^h(i) = f_h\left(\boldsymbol{D}'_k(i), \boldsymbol{D}\right), \tag{6}$$

where $i = 1, \cdots, \mathcal{L}$. The total predictions of multiple classifiers can be written as $\boldsymbol{z}_k(i) = \left[z_k^1(i), \cdots, z_k^H(i)\right]^T$.

The weights for multiple classifiers at the k-th grid point can be calculated by minimizing the following average positioning error

$$\begin{aligned} \boldsymbol{w}_k = \arg\min_{\boldsymbol{w}_k} & \frac{1}{\mathcal{L}} \sum_{i=1}^{\mathcal{L}} e\left(\boldsymbol{z}_k(i) \,|\boldsymbol{w}_k\right) \\ \text{s.t.} \quad & \boldsymbol{w}_k^T \boldsymbol{1} = 1, \\ & w_k(h) > 0, \end{aligned} \tag{7}$$

where the positioning error is given by

$$e\left(\boldsymbol{z}_k(i) \,|\boldsymbol{w}_k\right) = \left\|\boldsymbol{w}_k^T g\left(\boldsymbol{z}_k(i)\right) - g(k)\right\|_2^2, \tag{8}$$

where $g(\cdot) : \mathcal{R}^1 \rightarrow \mathcal{R}^2$ is a function which maps a label to the corresponding 2-D coordinate. The total weights matrix $\boldsymbol{W} = [\boldsymbol{w}_1, \cdots, \boldsymbol{w}_K]$ can be obtained by solving Eq. (7).

C. Online Localization

In the online phase, assume that we measure a joint geomagnetism and RSS testing sample $\tilde{\boldsymbol{d}} \in \mathcal{R}^L$, we can calculate the Euclidean distances between $\tilde{\boldsymbol{d}}$ and the offline fingerprints $\boldsymbol{D}$ as

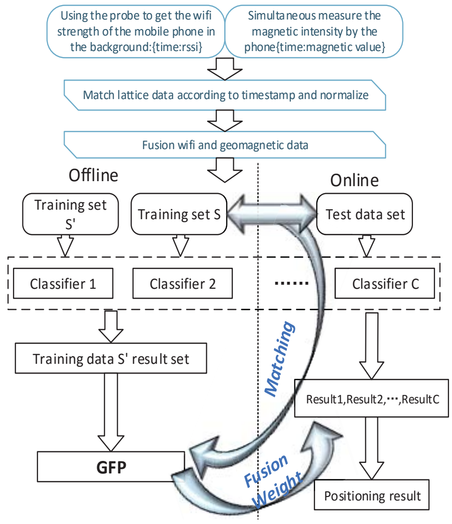

Fig. 3: Overview of our proposed localization approach.

$$\hat{o}_k = \left\|\tilde{\boldsymbol{d}} - \bar{\boldsymbol{D}}_k\right\|_2, \tag{9}$$

where $\bar{\boldsymbol{D}}_k$ is the mean of $\boldsymbol{D}_k$ at the k-th grid point. The best matched index of the grid point can be given by

$$\left[\text{value}, \hat{k}\right] = \min \hat{\boldsymbol{o}}, \tag{10}$$

in which $\hat{\boldsymbol{o}} = [\hat{o}_1, \cdots, \hat{o}_K]^T$. The actual outputs of multiple classifiers when given the online testing $\tilde{\boldsymbol{d}}$ are

$$\tilde{\boldsymbol{z}} = \left[f_1\left(\tilde{\boldsymbol{d}}, \boldsymbol{D}\right), \cdots, f_H\left(\tilde{\boldsymbol{d}}, \boldsymbol{D}\right)\right]^T \tag{11}$$

The final fusion positioning estimate can be calculated by

$$\hat{z} = \hat{\boldsymbol{w}}_{\hat{k}}^T g(\tilde{\boldsymbol{z}}). \tag{12}$$

IV. Experimental Results

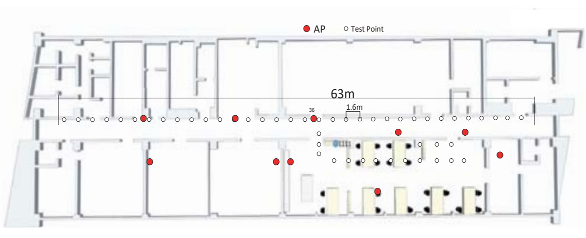

Fig. 4: The experiment environment.

To test the fusion performance of our proposed method, four typical machine learning algorithms, k-nearest neighbor (KNN) [21], support vector machine (SVM) [22], linear discriminant analysis (LDA) and random forest (RF) [3] as multiple classifiers. The experimental environment is shown as Fig. 4. The positioning area is 58.2m x 18.6m. The red dots represent the positions of the APs, the white hollow circle dots are the grid points of collecting samples, and the distance between adjacent grid points is 1.6m. We collect 100 and 50 offline fingerprints by Redmi note 4X at 50 grid points for classifiers and weights training, respectively, i.e., $Q = 100$. For simplicity, here and in the sequel, we denote our proposed method as GFP for comparison.

First, we compare the performance of different algorithms with normalized fingerprints and non normalized fingerprints. Table I shows that different methods show different improvements after normalization.

TABLE I: Mean root mean squared errors (RMSEs) of different algorithms by no normalization and normalization data

Algorithms	Mean RMSEs (m)	
	No normalization	Normalization
GFP	0.9266	0.8241
DCF	0.9550	0.8570
MMSE	0.9891	0.8599
KNN	1.0745	1.0232
SVM	1.0902	0.9472
LDA	1.2405	1.2405
RF	1.2809	1.1589

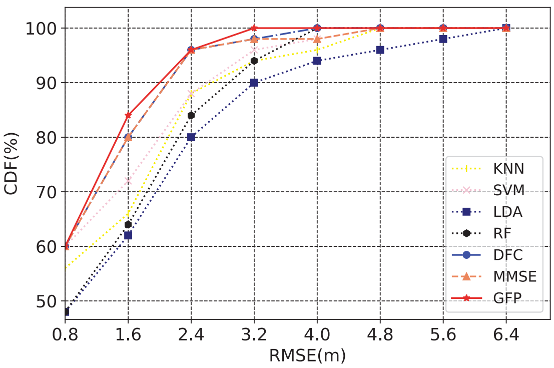

Fig. 5: The CDF of RMSE based on WiFi and magnetism fingerprints.

Fig. 5 shows the cumulative distribution function (CDF) of RMSE. It shows that the probability of GFP in acquiring RMSE of less than 1.6m is 84%, and DFC and MMSE is up to 80%, while machine learning methods KNN, SVM, LDA, RF are 66%, 72%, 62%, 64% respectively. We can find that our proposed method outperforms other methods in positioning accuracy.

Fig. 6 illustrates the RMSEs at all the test grid points. From this figure, we can find that our proposed GFP is more robust than other methods because the RMSEs at most grid points are no more than 2m.

Fig. 7 shows the performance difference by using WiFi and geomagnetism fingerprints and only WiFi fingerprints, which shows that the former reduces the mean RMSE by 35.0%

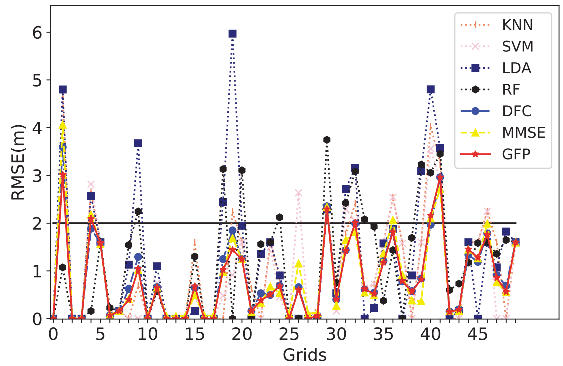

Fig. 6: RMSEs of different grids in positioning based on WiFi and geomagnetism.

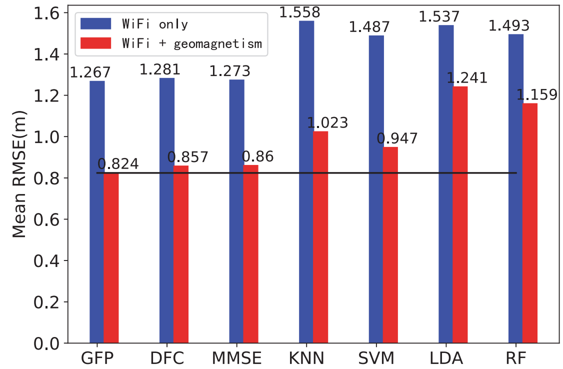

Fig. 7: Comparison of mean error.

33.1% 32.4% 34.3% 36.3% 19.3% 22.4% responding to GFP, DFC, MMSE, KNN, SVM, LDA, RF, as compared with the latter.

V. Conclusion

In this paper, we have proposed a multiple classifiers global dynamic fusion location system based on WiFi and geomagnetism. In the offline phase, firstly, a preprocessing method is used to align the two heterogeneous fingerprints. Then, several independent machine learning algorithms are selected to train multiple classifiers, and the global weighted matrix for each grid point is obtained through global supervised optimization learning. In the online phase, the final fusion coordinate position is obtained according to the global dynamic fusion algorithm. Simulation results verify the efficacy of our proposed system.

Acknowledgment

This work has been supported in part by the National Natural Science Foundation of China under Grant (No. 61371184, No. 61671137, No. 61771114) and the Fundamental Research Funds for the Central Universities (No. ZYGX2016J028).

References

[1] A. H. Salamah, M. Tamazin, M. A. Sharkas, and M. Khedr, “An enhanced WiFi indoor localization system based on machine learning,” in *Proc. IEEE IPIN*, 2016, pp. 1–8.

[2] J. Zhang, J. Sun, H. Wang, W. Xiao, and L. Tan, “Large-scale WiFi indoor localization via extreme learning machine,” in *Proc. CCC*, 2017, pp. 4115–4120.

[3] X. Guo, N. Ansari, L. Li, and H. Li, “Indoor localization by fusing a group of fingerprints based on random forests,” *IEEE Internet Things J.*, vol. PP, no. 99, pp. 1–1, 2018.

[4] W. Zhang, R. Sengupta, J. Fodero, and X. Li, “DeepPositioning: Intelligent fusion of pervasive magnetic field and WiFi fingerprinting for smartphone indoor localization via deep learning,” in *Proc. ICMLA*, 2017, pp. 7–13.

[5] X. Guo, L. Chu, and X. Sun, “Accurate localization of multiple sources using semidefinite programming based on incomplete range matrix,” *IEEE Sensors J.*, vol. 16, no. 13, pp. 5319–5324, 2016.

[6] X. Guo, L. Chu, and N. Ansari, “Joint localization of multiple sources from incomplete noisy euclidean distance matrix in wireless networks ,” *Comput. Commun.*, vol. 122, pp. 20–29, 2018.

[7] G.-y. Jin, X.-y. Lu, and M.-S. Park, “An indoor localization mechanism using active RFID tag,” in *Proc. IEEE SUTC*, vol. 1, 2006, pp. 4–pp.

[8] U. Bolat and M. Akcakoca, “A hybrid indoor positioning solution based on Wi-Fi, magnetic field, and inertial navigation,” in *Proc. IEEE WPNC*, 2017, pp. 1–6.

[9] S. Dudley-McEvoy, “UWB localization employing supervised learning method,” *Proc. ICUWB*, pp. 1–5, 2017.

[10] F. Ijaz, H. K. Yang, A. W. Ahmad, and C. Lee, “Indoor positioning: A review of indoor ultrasonic positioning systems,” in *Proc. IEEE ICACT*, 2013, pp. 1146–1150.

[11] Z. Chen, Q. Zhu, and Y. C. Soh, “Smartphone inertial sensor-based indoor localization and tracking with iBeacon corrections,” *IEEE Trans. Ind. Informat.*, vol. 12, no. 4, pp. 1540–1549, 2016.

[12] X. Guo, S. Shao, N. Ansari, and A. Khreishah, “Indoor localization using visible light via fusion of multiple classifiers,” *IEEE Photon. J.*, vol. 9, no. 6, pp. 1–16, 2017.

[13] X. Guo and N. Ansari, “Localization by fusing a group of fingerprints via multiple antennas in indoor environment,” *IEEE Trans. Veh. Technol.*, vol. 66, no. 11, pp. 9904–9915, 2017.

[14] S.-H. Fang, Y.-T. Hsu, and W.-H. Kuo, “Dynamic fingerprinting combination for improved mobile localization,” *IEEE Trans. Wireless Commun.*, vol. 10, no. 12, pp. 4018–4022, 2011.

[15] X. Guo, L. Li, N. Ansari, and B. Liao, “Knowledge aided adaptive localization via global fusion profile,” *IEEE Internet Things J.*, vol. 5, no. 2, pp. 1081–1089, 2017.

[16] ——, “Accurate wifi localization by fusing a group of fingerprints via global fusion profile,” *IEEE Trans. Veh. Technol.*, vol. PP, no. 99, pp. 1–1, 2018.

[17] F. Evennou and F. Marx, “Advanced integration of WiFi and inertial navigation systems for indoor mobile positioning,” *Eurasip journal on applied signal processing*, vol. 2006, pp. 164–164, 2006.

[18] R. Kang and L. Cao, “Smartphone indoor positioning system based on geomagnetic field,” in *Proc. CAC*. IEEE, 2017, pp. 1826–1830.

[19] W. Shao, F. Zhao, C. Wang, H. Luo, T. Muhammad Zahid, Q. Wang, and D. Li, “Location fingerprint extraction for magnetic field magnitude based indoor positioning,” *Journal of Sensors*, vol. 2016, 2016.

[20] E. Le Grand and S. Thrun, “3-axis magnetic field mapping and fusion for indoor localization,” in *Proc. IEEE MFI*, 2012, pp. 358–364.

[21] T. Cover and P. Hart, “Nearest neighbor pattern classification,” *IEEE Trans. Inf. Theory*, vol. 13, no. 1, pp. 21–27, 1967.

[22] J. A. Suykens and J. Vandewalle, “Least squares support vector machine classifiers,” *Neural processing letters*, vol. 9, no. 3, pp. 293–300, 1999.